Influence of antecedent soil moisture conditions on the synoptic meteorology of the Black Saturday bushfire event in southeast Australia

Jatin Kala*, Jason P. Evans and Andy J. Pitman

Australian Research Council Centre of Excellence for Climate Systems Science and Climate Change Research Centre, University Of New South Wales, Sydney, New South Wales, Australia

*Correspondence to: Jatin Kala, Climate Change Research Centre, Level 4, Matthews building, University Of New South Wales, Email: J.Kala@unsw.edu.au or Jatin.Kala.JK@gmail.com

The dynamics and large-scale drivers of heat wave (HW) events in Australia are well documented. However, the influence of soil moisture in modulating HWs is largely unexplored. We focus here on a recent significant HW event in southeast Australia that preceded the Black Saturday bushfires (3rd to the 7th of February 2009). During this period, the southeast of Australia experienced unprecedented warm conditions, which, in conjunction with high fuel load and mesoscale weather conditions, led to devastating bushfires. We examine how different initial soil moisture conditions with lead times of 5, 10, and 15 days prior to the event would have altered its overall dynamics at the continental scale. We show that at short lead times (5 days), the influence of perturbing soil moisture is mostly linear. Decreasing (increasing) soil moisture increases (decreases) maximum temperatures, associated with an intensification of the upper-level anticyclone. The effect of increasing soil moisture is more non-linear than decreasing soil moisture with increasing lead time; namely, increasing soil moisture can also lead to an increase in maximum temperature over some parts of the domain, rather than a decrease everywhere. At lead times of up to 15 days, the imposed perturbation in soil moisture, mostly confined to the tropics, is essentially lost such that the impact on maximum temperatures on the day of the event cannot be related to the sign of the imposed perturbation in soil moisture. Our results highlight the importance of accurate soil moisture estimates in capturing the intensity and spatial extent of HW events in southeast Australia, but only at relatively short lead times.

Key Words: extreme heat; heat waves; land-atmosphere feedback; soil moisture; WRF

 Prepared using qjrms4.cls

Received . . .

1. Introduction

During the summer of 2008-2009, southeast Australia experienced unprecedented extreme heat conditions with maximum temperatures reaching 46.8°C, culminating with catastrophic bushfires on the 7th of February 2009 (the Black Saturday bushfires), with a maximum temperature anomaly of up to +18°C (Jacobs *et al.* 2014). These bushfires caused significant damage to infrastructure estimated to be more than $4 billion and resulted in 173 human fatalities (Teague *et al.* 2010). Heat wave (HW) conditions were observed up to 2 weeks prior to the event, with nine out of the eleven preceding days exceeding 30°C (Engel *et al.* 2013). This event was largely driven by mesoscale atmospheric dynamics, including complex interactions involving a late-afternoon cold front and propagating nocturnal bores (Engel *et al.* 2013).

Several studies have attempted to link the occurrence of HWs in Australia to various modes of climate variability and a range of hypotheses have been suggested. Cai *et al.* (2009) showed that extreme bushfire conditions, such as those experienced during the Black Saturday bushfires, tend to be preceded by positive Indian Ocean Dipole (IOD) events. These tend to produce lower than average rainfall and higher temperatures over eastern Australia, which exacerbate dry conditions. Marshall *et al.* (2014) focussed on intra-seasonal drivers of HWs in Australia and showed that there is skilful predictability of increases in heat extremes with lead times of up to 2-3 weeks with the negative phase of the Southern Annular mode (SAM), the vicinity of the sub-tropical ridge, and the Madden-Julian Oscillation (MJO). Parker *et al.* (2014b) on the other hand link southeastern Australian HWs to distinct phases of the MJO and the La Nina phases of the El Niño Southern Oscillation (ENSO), but could not link the frequency of HWs to the phases of SAM.

Several studies have also investigated teleconnections which act to reinforce HW-like conditions. Using a tracking scheme, Pezza *et al.* (2011) showed that a pressure dipole formed by transient cyclones and anticyclones can reinforce HWs in southern Australia. They also show that that HWs over eastern Australia tend to be associated with enhanced monsoon seasons over northern Australia as compared to HWs occurring over Western Australia. Similar teleconnections have been established elsewhere, for example the 2010 Pakistan floods and Russian HWs are thought to have been inter-connected (Lau and Kim 2012). Martius *et al.* (2013) focussed on the same event and highlighted the role of evapotranspiration from the land surface in increasing atmospheric humidity. A study by Parker *et al.* (2013) has shown that HWs in southeast Australia, in particular, the Black Saturday event was strongly influenced by the interaction between a tropical cyclone and the large-scale midlatitude flow. A more detailed analysis HWs affecting southeastern Australia by Parker *et al.* (2014a) further highlights the strong connections between heavy rainfall over the northeast and HWs in southeast Australia.

Few studies have explicitly examined the role of soil moisture on HW dynamics in Australia. Jones and Trewin (2000) showed that variations in large-scale soil moisture associated with rainfall changes due to the ENSO can enhance the seasonal predictability of land surface temperatures in Australia. Other studies have focussed on the role of soil moisture on climate variability and shown that it is not possible to capture atmospheric variability over Australia without resolving soil moisture variability (Timbal *et al.* 2002). Nicholls and Larsen (2011) investigated the effect of long-term droughts on temperature extremes in southeast Australia and showed that daily maximum temperatures are typically 1-3 °C higher after droughts, such as the drought affecting southeast Australia prior to the Black Saturday bushfires. More broadly, Hirsch *et al.* (2014) have shown that realistic initial soil moisture conditions improves the predictability of maximum temperatures over Australia, especially at short lead times of 16-30 days.

The influence of soil moisture on HW dynamics has been examined elsewhere, especially for the 2003 European summer HWs. For example, Ferranti and Viterbo (2006) conducted simulations over this period and showed that the atmospheric response to large perturbations in soil moisture in the root zone lasted up to 2 months, while perturbations to the whole column increased the magnitude of the atmospheric response and lasted up to 3 months. These responses were larger than comparable ocean boundary forcing, and they hence argued that perturbing initial soil moisture conditions is a valuable tool in generating seasonal forecast ensembles. Fischer *et al.* (2007) examined a similar issue by perturbing soil moisture conditions leading into the

summer of 2003. They found that without imposing soil moisture anomalies, the European summer heat anomalies would have been reduced by up to 40% in some regions, and identified a positive feedback mechanism between soil moisture, continental scale circulation, and temperature. Specifically, drier soils intensify anticyclone circulation anomalies, leading to higher temperatures. Similar mechanisms are reported by Zampieri *et al.* (2009) who investigated the role of soil moisture on European HWs (including the 2003 event) and showed that drier soils led to higher emissions of sensible heat and favor upper-air anticyclonic circulations.

Several studies have focused on the influence of soil moisture anomalies on the magnitude of HW events. Lorenz *et al.* (2010) investigated the influence of soil moisture memory on HW persistence and found that simulations with prescribed soil moisture had lower intrinsic HW persistence as compared to simulations with interactive (freely evolving) soil moisture. These modeling results have also been confirmed by observational studies (Hirschi *et al.* 2010) of soil moisture-atmosphere feedbacks over southeastern Europe using station observations. Hirschi *et al.* (2010) also noted that while models correctly simulated the soil moisture-atmosphere feedback, they tend to overestimate this feedback over central Europe. A more recent observational study of the 2003 and 2010 European HWs showed that the increased desiccation of the land surface via the advection of heat from large-scale systems acted to progressively accumulate heat within the atmospheric boundary layer over several days, eventually leading to mega-HW events (Miralles *et al.* 2014).

Finally, Stéfanon *et al.* (2012) investigated soil moisture-temperature feedbacks over France between 1989 and 2008 using a regional climate model with two different land surface models, one with dynamic hydrology and able to simulate summer dryness, and the other with a constant high soil moisture and no deficit. They found the response of the atmosphere varied with geography. In coastal areas, drier soils enhanced the sea-breeze circulation, which caused a cooling effect. In mountainous regions, drier soils enhanced sensible heating, which increased convection triggering. This led to more precipitation and a reduction in the temperature anomaly. Finally, over low elevation plains, drier soils led to higher sensible heat flux, lower evapotranspiration and a slight increase in shallow clouds, which led to higher temperatures. Hence, unlike previous studies, this study suggests that local effects play an important role in modulating temperature anomalies.

In summary, a large body of literature on the dynamics of HW events, especially for central Europe (e.g., Fischer *et al.* 2007; Zampieri *et al.* 2009; Hirschi *et al.* 2010; Lorenz *et al.* 2010; Stéfanon *et al.* 2012; Miralles *et al.* 2014) shows that soil moisture-atmosphere interactions are important. Whilst the dynamical meteorology of the Black Saturday bushfires event is well documented (Engel *et al.* 2013) and the overall large-scale drivers of bushfire weather in Australia have been extensively studied (e.g., Cai *et al.* 2009; Pezza *et al.* 2011; Parker *et al.* 2013; Boschat *et al.* 2014; Cowan *et al.* 2014; Marshall *et al.* 2014; Purich *et al.* 2014; Parker *et al.* 2014b), there is a clear knowledge gap on the role of soil moisture-atmosphere feedbacks for Australian HWs and associated bushfire events. This paper aims to address this knowledge gap by focusing on the HW conditions during the Black Saturday bushfires as a case study, with emphasis on the role of soil moisture on the synoptic meteorology of the event.

2. Methods

2.1. *Simulations*

We used the Weather Research and Forecasting system (WRF) Advanced Research WRF (WRF-ARW) Version 3.5 (Skamarock *et al.* 2008), driven with 6-hourly boundary conditions from ERA-Interim (Dee *et al.* 2011) over the Australian domain as specified by the Coordinated Regional Downscaling Experiment (CORDEX, Giorgi *et al.* 2009), shown in Figure 1 (50 km resolution). We used the same WRF physics setting as Evans and McCabe (2010), which produces a reasonable climatology over southeast Australia, with maximum biases in the mean seasonal temperature and precipitation of approximately $\pm 2^{o}$C and -50 to +10 mm month^{-1} respectively, which were mostly confined to regions of complex topography. The model has also been shown to simulate diurnal rainfall variably over southeast Australia reasonably well (Evans and Westra 2012) and similar results have been reported over Western Australia using the same

WRF physics settings (Kala *et al.* 2015; Andrys *et al.* 2015). The control (CNTL) simulation was carried out by initialising the model on the 1st of October 2008, providing a 4-month model-spin prior to the event on the 7th of February 2009. All simulations used the NOAH land surface model (Ek 2003).

To investigate the influence of antecedent soil moisture conditions, simulations were conducted that increased and decreased the soil moisture across all model soil levels, by ± 5%, 15%, and 25% percent, at 5, 10, and 15 days lead time to the 7th of the February 2009, using restart files from the CNTL experiment. The initial soil moisture fields at each of these lead times (Figure 2) show a clear soil moisture gradient between the northern tropical region and the rest of the continent, which was mostly dry. The imposed changes in soil moisture therefore acted to reduce or intensify that gradient.

The choice of 5, 10, and 15 days lead time was made since weather forecasts are generally made over these timescales. Our experiments therefore indirectly inform how accurate soil moisture initialisation needs to be, to capture HW events such as the Black Saturday event. While previous studies that have investigated the influence of soil moisture on HWs have restricted the perturbation to soil moisture within the wilting point and field capacity range (e.g., Zampieri *et al.* 2009), we did not apply such a constraint. This is illustrated in Figure 3 showing the percentage difference in surface soil moisture between the experiments with reduced soil moisture and the wilting point soil moisture, and experiments with increased soil moisture and the field capacity soil moisture, at each of the different lead times. Surface soil moisture for the experiments with reduced soil moisture falls below the wilting point over the centre of the continent (±10%) for all experiments, especially when the largest perturbation of -25% percent is applied. This represents a large perturbation; soil moisture below wilting point implies vegetation cannot transpire but this is not an unrealistic situation over a semi-arid continent such as Australia. Similarly, surface soil moisture for the experiments with increased soil moisture exceeds the field capacity over the northern tropical regions (±10%), especially for the experiments with +25% perturbation. This implies that any excess soil moisture would be lost via surface runoff. Again, this is also not an unrealistic assumption over these regions, particularly during the monsoon season.

2.2. *Datasets*

We used the Australian Water Availability Project (AWAP) (Jones *et al.* 2009) gridded temperature and precipitation observations to evaluate the control simulation 2-m maximum temperatures (TMAX) and precipitation. The AWAP dataset has a resolution of 0.05^{o} by 0.05^{o} and is an interpolation from a network of weather stations across Australia, and has been previously used for evaluating regional climate simulations over Australia (Evans and McCabe 2010; Evans *et al.* 2012; Kala *et al.* 2015; Andrys *et al.* 2015). The AWAP data was interpolated to the coarser model grid using simple inverse distance weighting prior to comparisons.

Since this study investigates the influence of soil moisture, we also compared the model-simulated surface soil moisture with estimates from the Advanced Microwave Scattering Radiometer - Earth Observing System (AMSR_E) satellite product. The version of AMSR_E used in this study is described in Liu *et al.* (2009). While the AMSR_E product has inherent uncertainties, it should provide more realistic estimates of the overall spatial distribution of soil moisture as compared to a model-simulated soil moisture, as the latter strongly depends on accuracy of the model-simulated precipitation and evapotranspiration. Therefore we use the AMSR_E data to examine if the model simulates the overall magnitude and spatial distribution of surface soil moisture.

3. Results

3.1. *Model evaluation*

We first evaluate the control (CNTL) simulation of TMAX on the 7th of February 2009 along with the 5 day period to the peak of the event (3rd to the 7th of February 2009) since HW-like conditions were observed during the week prior to the event. The simulated TMAX are compared against gridded observations from the AWAP dataset, shown in Figure 4 (a) and (b) respectively. On the most extreme day of the event (7th of February 2009) WRF captures the overall spatial pattern of the HW event well (Fig. 4 (a)). There is a large negative bias in TMAX at the southeast coast of -10^{o}C to -12^{o}C, showing that the model-simulated HW did not

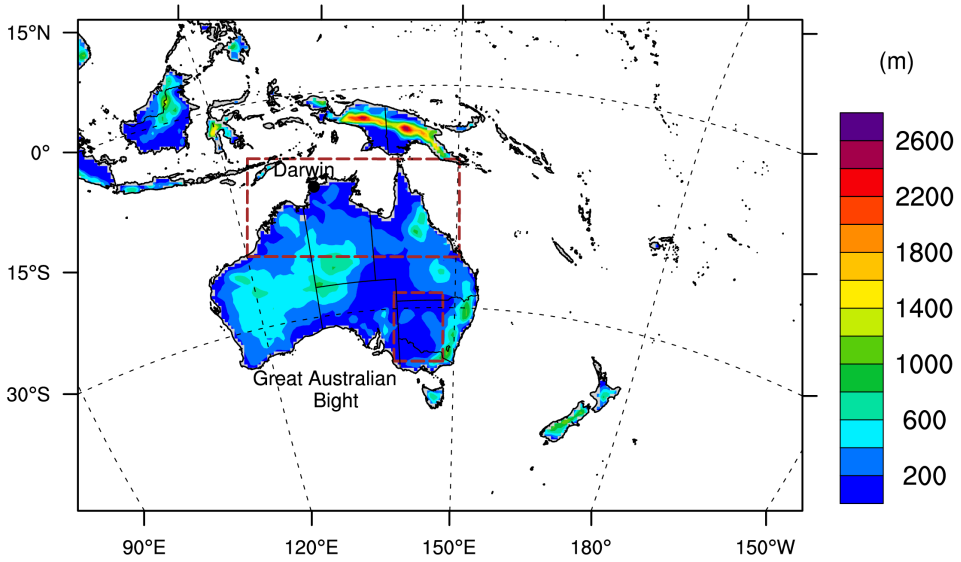

Figure 1. Topography (m) over the 50 km Coordinated Regional Downscaling Experiment (CORDEX) Australian domain used for the simulations. The boxes with dotted brown lines represents the regions used for the time-series plots in Figures 13 and 14. The black dot at -12.5°S, 130.9°E shows the location of city of Darwin.

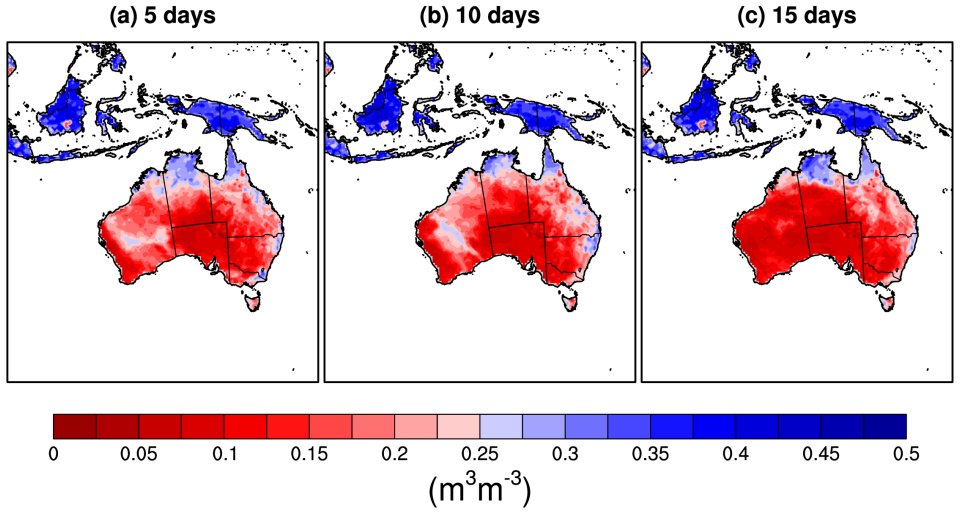

Figure 2. Surface soil moisture from the CNTL simulation at (a) 5 days, (b) 10 days, and (c) 15 days lead time to the 7th of February 2009.

extend as close to the coast as observed, as well as a positive bias of +4°C to +6°C in northeastern Australia. This is also reflected in the simulated TMAX over the 5 days to the peak of the event (Fig. 4 (b)). WRF under-estimates TMAX over the southeast and southwest by a smaller magnitude of -4°C to -8°C, but the overestimation over the northern part of the continent remains unchanged. These biases are considerably larger in magnitude as compared to those reported by Evans and McCabe (2010) ($\pm 2^{\circ}$C), who used the same WRF configuration over southeast Australia. However, the biases reported by the latter are for the mean seasonal temperature averaged over 24 years, whereas we focus on the bias in TMAX for one of the mostly significant HW events in history and larger errors are therefore to be expected. Finally, the focus of this paper is on the effects of soil moisture at the continental/synoptic scale and although the biases are large, the overall spatial structure of the simulated HW is satisfactory to warrant further simulations with perturbed soil moisture.

The observed (AWAP) and WRF simulated precipitation from the 1st of December 2008 to the 7th of February 2009 (i.e., summer precipitation prior to the event) and the difference between WRF and AWAP (WRF-AWAP) are shown in Figure 5. WRF under-estimates precipitation over the northern tropics by as much as 15 $\mathrm{mm\ day^{-1}}$, (corresponding to about 40% to 60% in percentage bias) but elsewhere the precipitation is close to observed. Shown in Figure 6 is a comparison of AMSR_E derived surface soil moisture, and WRF surface soil moisture over the same period. WRF captures the overall spatial patterns and magnitude of AMSR_E soil moisture well, although there are some distinct features which are not reproduced by the model. WRF simulates lower soil moisture than the AMSR_E over the

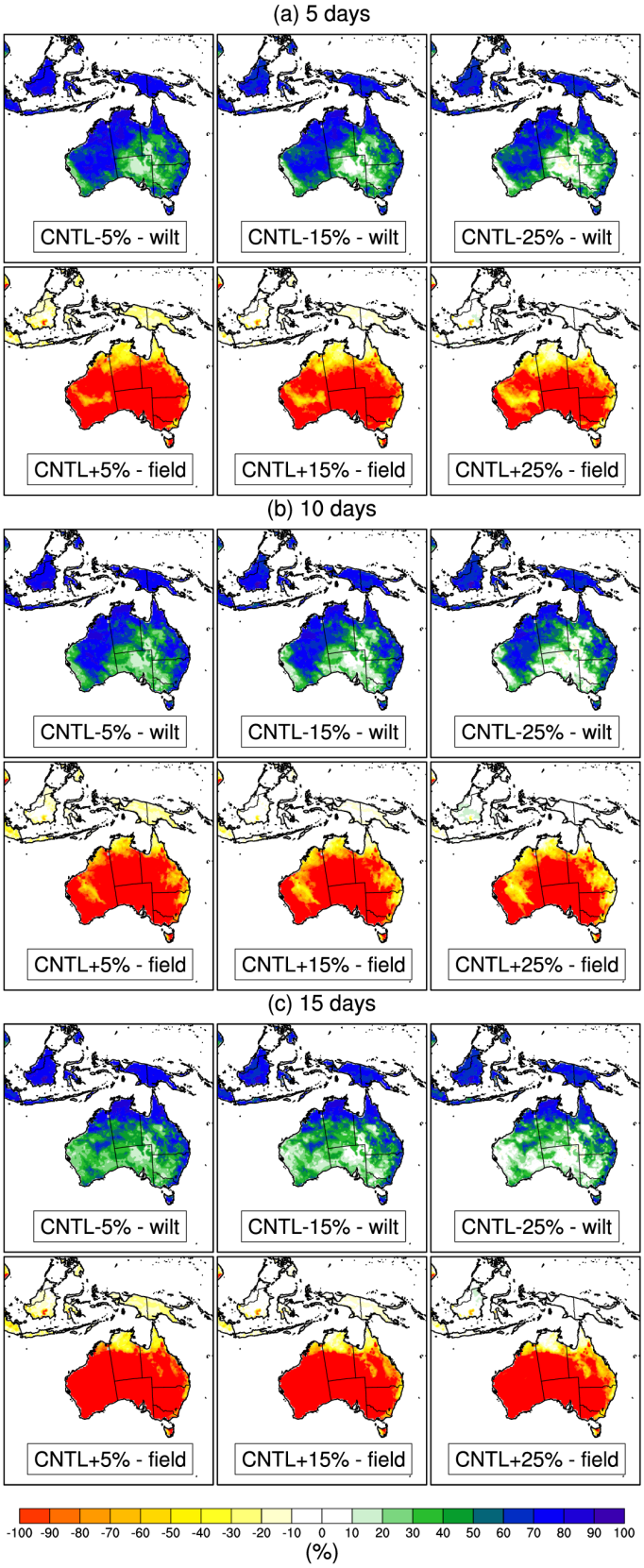

Figure 3. Percentage difference in surface soil moisture between the experiments with -5, -15, and -25% and the wilting point soil moisture, i.e., ((experiment-wilting_point)/experiment)×100 (top panels), and +5, +15, and +25% and field capacity, i.e., ((experiment - field_capacity)/experiment)×100, (bottom panels) for (a) 5 days, (b) 10 days, and (c) 15 days lead time to the 7th of February 2009. A positive value for the experiments with reduced soil moisture (top panels) indicates that perturbed soil moisture was higher than the wilting point soil moisture and a negative value for the experiments with increased soil moisture (bottom panels) indicates that the perturbed soil moisture was lower than field capacity.

northern tropics, which can be related to WRF under-estimating precipitation over the same region. There are also large negative differences over Tasmania and the southeast and southwestern coasts. However, these areas are densely vegetated and AMSR_E estimates are likely to be less accurate. WRF generally has higher soil moisture over the center of the continent compared to AMSR_E by about 0.025 $\mathrm{m}^3\ \mathrm{m}^{-3}$ to 0.075 $\mathrm{m}^3\ \mathrm{m}^{-3}$. This is within the wilting point soil moisture used within the NOAH

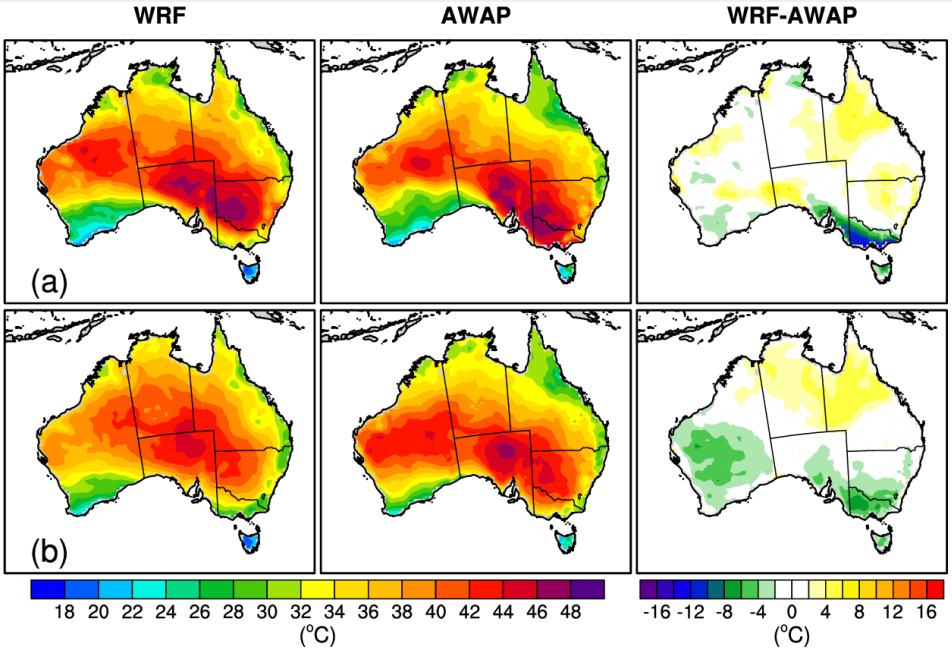

Figure 4. Comparison between WRF simulated and AWAP observed maximum temperature for the control (CNTL) experiment on (a) the 7th of February 2009 (daily maximum), and (b) between the 3rd and the 7th of February 2009 (i.e., mean over the 5 day period to the peak of the event).

land surface scheme over Australia, which varies between 0.02 $m^3\ m^{-3}$ and 0.1 $m^3\ m^{-3}$. Overall, the general pattern of WRF simulated soil moisture as compared to AMSR_E is satisfactory to warrant using the model for further simulations with perturbed soil moisture conditions.

3.2. *Sensitivity to soil moisture*

Figure 7 shows the difference in 2-m maximum temperature (TMAX) between each experiment at the different lead times and the CNTL on the 7th of February 2009 (positive values imply that the experiment is warmer than the control and vice-versa). At 5 days lead time to the 7th of February 2009 (Fig. 7 (a)), decreasing (increasing) initial soil moisture by 25% increases (decreases) TMAX by about 2°C to 3°C. While the response of the model to decreased soil moisture is broadly consistent, i.e., decreased soil moisture leads to increased TMAX, there are instances when increasing soil moisture leads to an increase in TMAX. This is especially apparent for the ±25% experiment, which shows regions of both increases and reductions in TMAX over parts of the northern tropics and the southeast for the +25% experiment. We explore these dynamics in more detail later in the manuscript.

At 10 and 15 days lead time (Figures 7 (b) and (c)), a noticeable difference compared to 5 days lead time (Figure 7 (a)) is that the response of TMAX is larger with an increase in soil moisture compared to a decrease. The increase in TMAX with decreased soil moisture is approximately 2°C to 4°C, whereas the decrease in TMAX with increased soil moisture is approximately -2°C to -7°C. This can be expected over a mostly arid continent such as Australia, as the imposed reduction in soil moisture is essentially making an already dry continent drier, i.e., the ratio of sensible to latent heat is unlikely to change drastically. On the other hand, increasing soil moisture provides a mechanism for increased evaporation and hence a larger influence on the partitioning of available energy into latent heat which would reduce the ratio of sensible to latent heat, providing a mechanism for larger changes in TMAX. This is further explored later in the manuscript.

Another noticeable difference at 10 and 15 days lead time (Figures 7 (b) and (c)) as compared to 5 days (Figure 7 (a)), is that the response of the model to different initial soil moisture is increasingly less linear, especially when initial soil moisture is increased. Increasing soil moisture leads to both increases and decreases in TMAX within different regions of the domain. At 10 days lead time, increasing soil moisture by +5% leads to a decrease in TMAX over the west of the domain, which gradually increases in size as the perturbation is increased to +25%. At the same time, a region of increase in TMAX at the southeast corner of the domain gradually intensifies, which corresponds to the region where the CNTL simulation has the largest bias in TMAX (Figure 4). Interestingly, even at +5%, the increase in TMAX

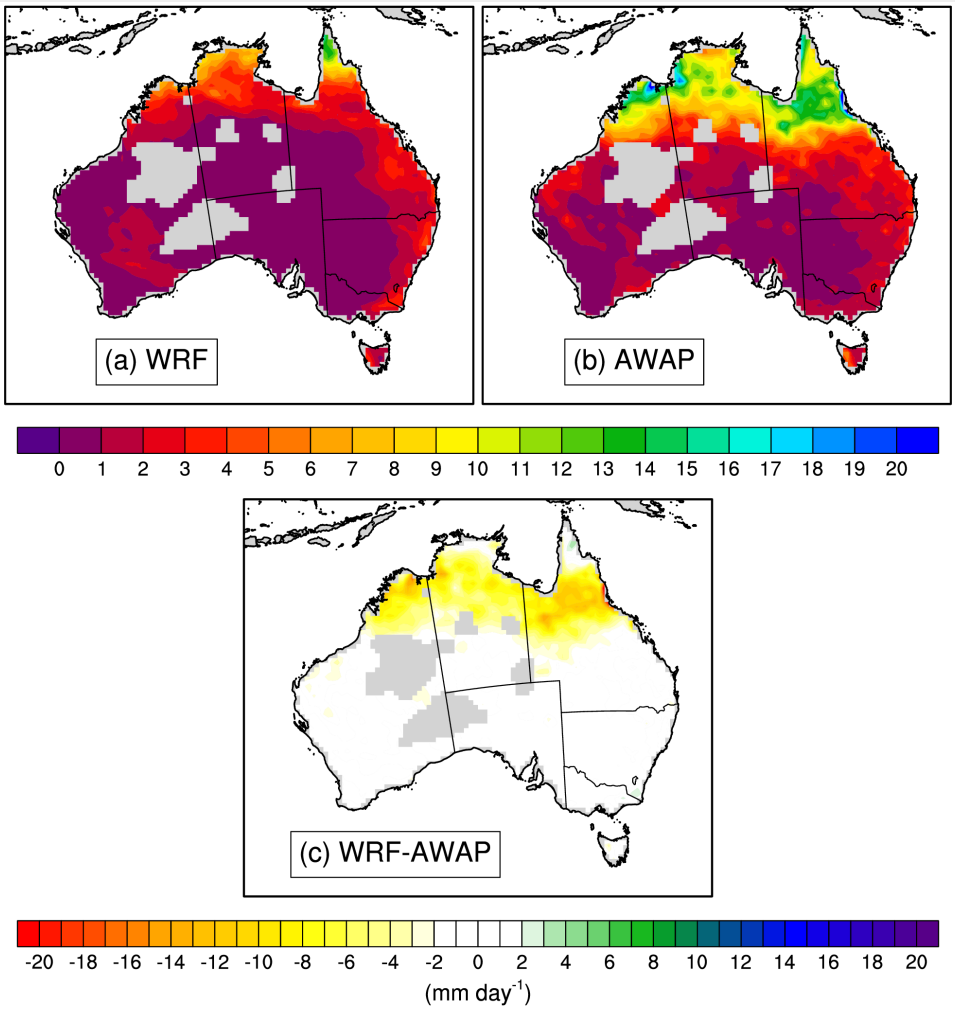

Figure 5. Comparison between (a) WRF, (b) AWAP total precipitation ($\mathrm{mm\ day^{-1}}$) from the 1st of December 2008 to the 7th of February 2009, and (c) the differences between WRF and AWAP (WRF-AWAP). Inland masked areas in grey are regions whereby AWAP gridded observations are not available.

covers large parts of the continent. The dynamics behind these unexpected results is further explored later in the manuscript.

At 15 days lead time, increasing soil moisture results in an increase in TMAX to the very north of the domain, which intensifies with increasing perturbation of increasing soil moisture from +5% to +25% (Fig. 7(c), bottom panels). At +5%, this extends over most of the domain but the intensification is restricted to the north. At the same time, there are large regions of decrease in TMAX over the southwest of the domain, especially for the +25% experiment. There are also decreases in TMAX to the east of the domain for the +15% and +25% experiments. Additionally, at 10 and 15 days lead time, the effect of decreasing soil moisture is less linear when the perturbation is small (i.e., there are regions of both increase and decrease in TMAX at -5% and -15%, but mostly only increases in TMAX at -25%). As was shown in Figure 3, it is at -25% that the imposed perturbation falls below the wilting point soil moisture, showing that a relatively large negative perturbation (i.e., decrease) in soil moisture needs to be applied to obtain a consistent increase in TMAX across the domain. Additionally we also note that surface soil moisture was slightly lower south of the northern tropics at 15 days lead time as compared to 5 and 10 days lead time for the CNTL (Fig. 2). Hence relatively small reductions in soil moisture of -5% to -15% applied at 15 days lead time are less likely to show a consistent increase in TMAX on the day of the event across the continent.

To determine whether the changes in TMAX on the 7th of February 2009 shown in Figure 7 could be due to internal model variability, we also show the same differences but averaged from the 3rd to the 7th of February (i.e., the preceding 5 days) in Figure 8. Although the magnitude of the differences is smaller compared to differences on the day of the event (Figure 7), the patterns are similar. At 5 days lead time, the influence of decreasing (increasing) soil moisture is largely linear and results in an increase (decrease) in TMAX. At 10 days lead time (Fig. 8 (b)), there is an increase in TMAX over the southeast when soil moisture is increased, similar in pattern to Figure 7 (b). At 15 days

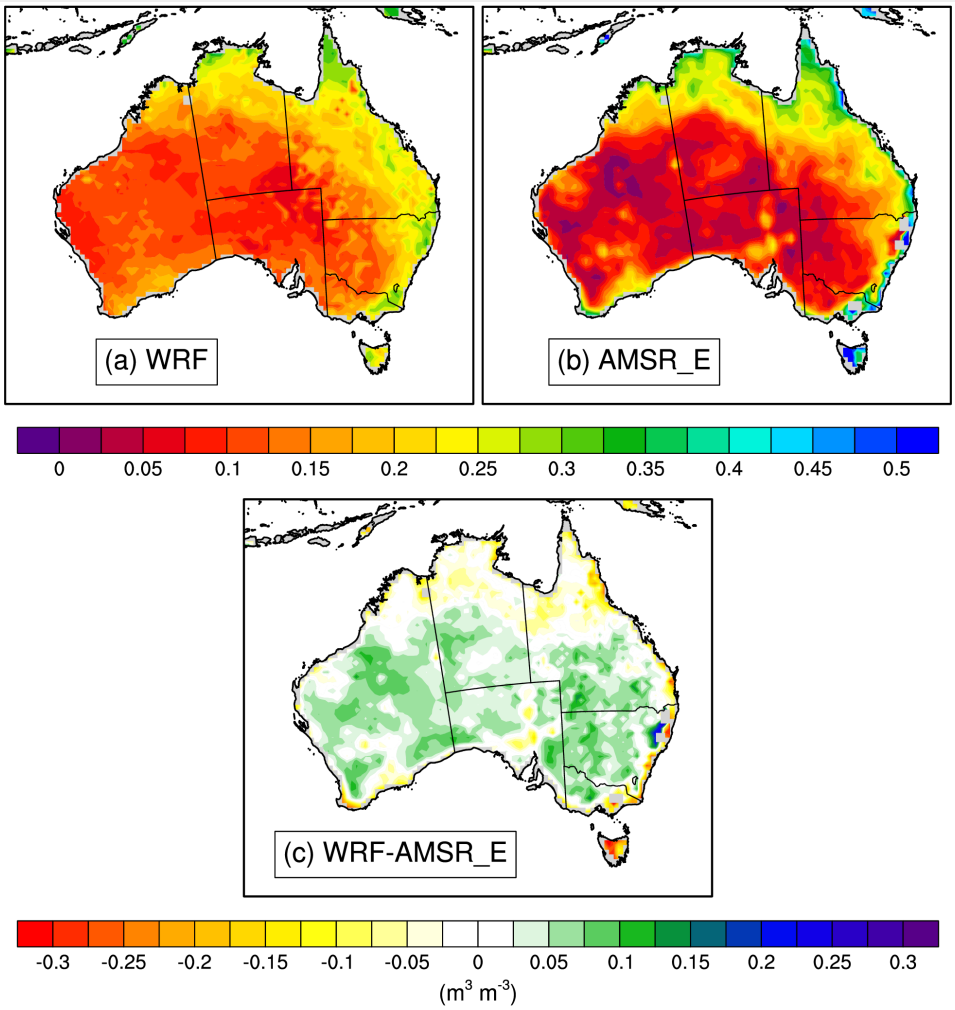

Figure 6. Comparison between (a) WRF, (b) AMSR_E surface soil moisture ($\mathrm{m}^3\ \mathrm{m}^{-3}$) from the 1st of December 2008 to the 7th of February 2009, and (c) the differences between WRF and AMSR_E (WRF-AMSR_E). Inland masked areas are regions whereby AMSR_E estimates are not available.

lead time the patterns are not as similar as with 10 days, but both simulations show regions of increase and decrease in TMAX with increasing initial soil moisture.

As discussed in the introduction, the main dynamical atmospheric response of reduced soil moisture leading to increased temperatures near the surface is an intensification of upper-level anticyclonic systems (Fischer *et al.* 2007; Zampieri *et al.* 2009). The mechanism proposed in the literature is that the enhanced sensible heat flux and associated reduced latent cooling leads to higher tropospheric air temperature which increases the thickness between the surface and 500 hPa. The enhanced surface heating due to the intensification of the upper-level anticyclone can therefore result in a positive feedback mechanism. To investigate this, we show the daily mean 500 hPa geopotential height (GPH) and the surface latent (Q_{le}) and sensible (Q_h) heat fluxes for the CNTL on the 7th of February 2009 in Fig. 9, and the difference between each experiment and the CNTL in Figs. 10 to 12.

Figure 9 (a) shows the presence of the upper-level anticyclone to the east, covering a large part of the center of the continent, north of the upper-level cyclone south of the Great Australian Bight. There is also a weak upper-level cyclone near Darwin (Fig. 1). The central interior of the continent was mostly dry with latent heat fluxes close to 0 $\mathrm{W\ m}^{-2}$ (Fig. 9 (b)) and sensible heat fluxes between 100 to 150 $\mathrm{W\ m}^{-2}$ (Fig. 9 (c)). Elsewhere, over the northern tropics, along the southeast Australian coast and central Western Australia, latent heat fluxes were between 100 to 150 $\mathrm{W\ m}^{-2}$ reflecting the average precipitation pattern (Fig. 5 (a)).

At 5 days lead time, there is a gradual increase in the 500 hPa GPH over the center of the continent as soil moisture is decreased from -5% to -25% (Fig. 10 (a), top panels), showing an intensification of the upper-level high. The opposite is true for the experiments with increased soil moisture and this can explain the overall increase (decrease) in TMAX with decreased (increased) soil moisture (Fig. 7 (a)). The increase (decrease) in 500 hPa GPH over the center of the continent is accompanied by a decrease

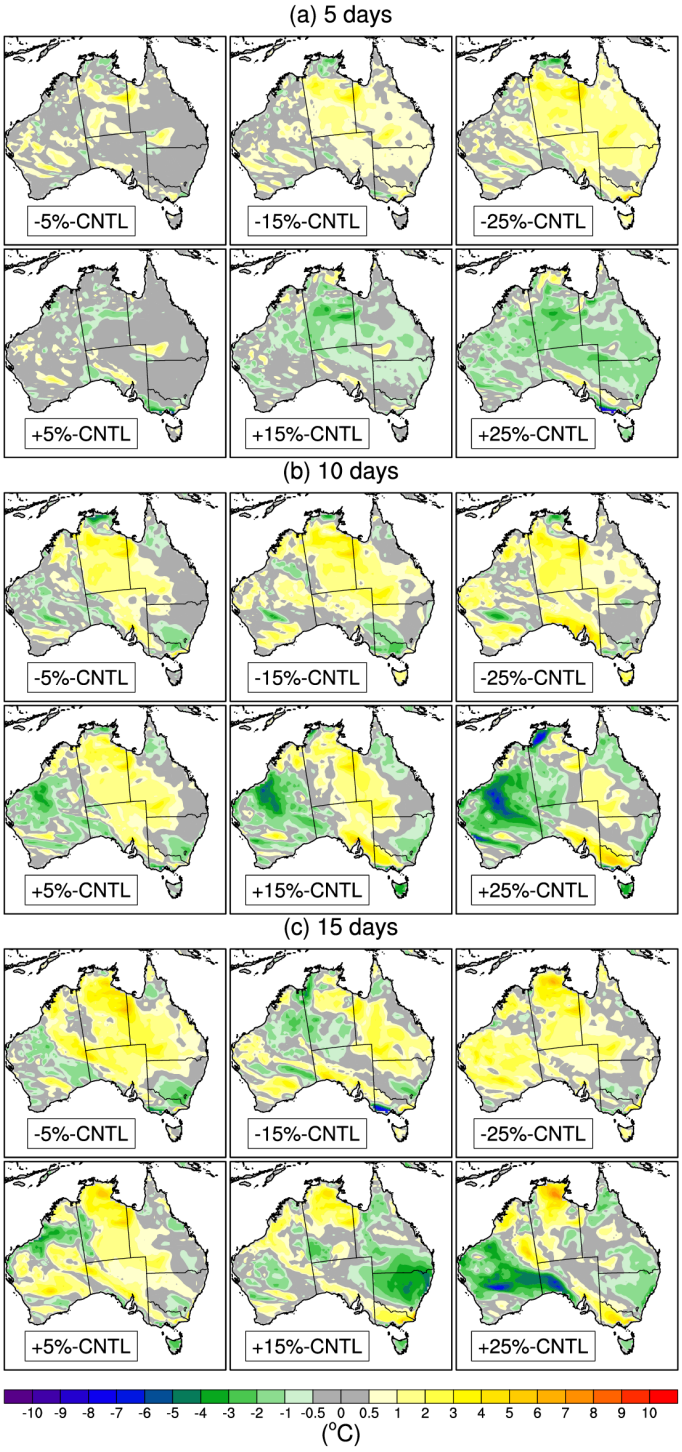

Figure 7. Difference in maximum 2 m temperature (TMAX) on the 7th of February 2009, between each experiment and the control (experiment-CNTL) started at (a) 5 days, (b) 10 days, and (c), 15 days lead time. Positive values indicate that the experiment was warmer than the control (CNTL) simulation.

(increase) in the 500 hPa GPH to the north of the continent near Darwin (Fig. 1) especially noticeable for the -25% experiment (Fig. 10 (a), top right panel (-25%-CNTL)). This can explain the decrease (increase) in TMAX with decreased (increased) soil moisture (Fig. 7 (a)) over this region (Fig. 7). There is also a gradual increase (decrease) in 500 hPa GPH over the ocean to the northeast of the continent and additionally, the experiments with increasing soil moisture also show an increase in 500 hPa GPH south of the Great Australian Bight (Fig. 10 (a), bottom panels). These changes in 500 hPa GPH over the ocean indicate that perturbing soil moisture over land not only influences the upper-level anticyclone over the continent, but this in turn influences the surrounding upper-level cyclonic systems. This "dipole-like" effect in the 500 hPa GPH has also been found by Fischer *et al.* (2007), especially when soil moisture in increased (see Fig. 8(c) of Fischer *et al.* (2007)).

To understand the drivers of the changes in the 500 hPa GPH, we examined the changes in the surface heat fluxes as shown in

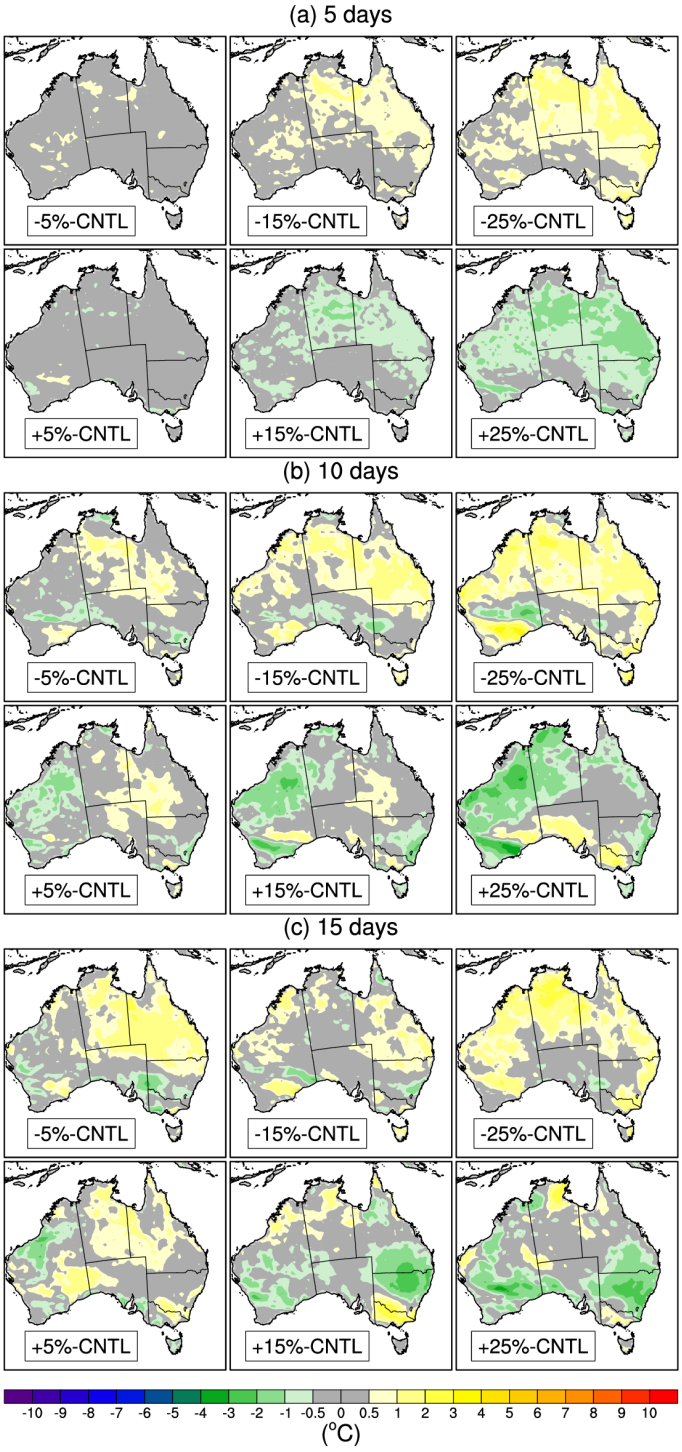

Figure 8. Same as in Figure 7, except averaged between the 3rd and the 7th of February 2009 (i.e., mean over the 5 day period to the peak of the event).

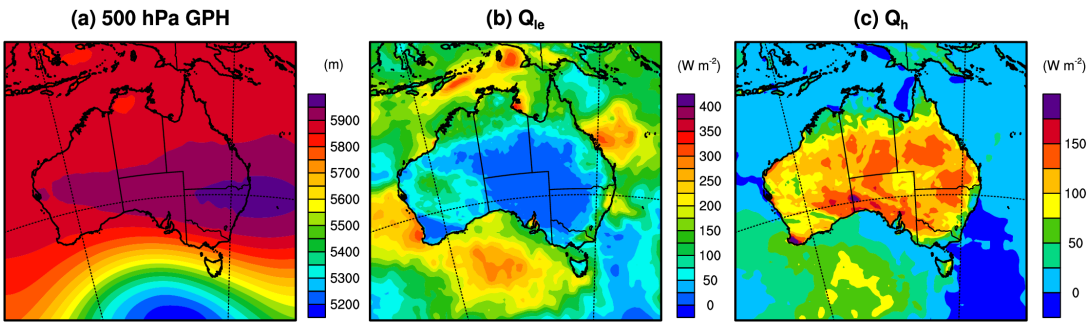

Figure 9. (a) Mean 500 hPa geopotential height (GPH, m), (b) surface latent heat flux (Q_{le} W m^{-2}), and (c) surface sensible heat flux (Q_h, W m^{-2}) for the control (CNTL) simulation on the 7th of February 2009.

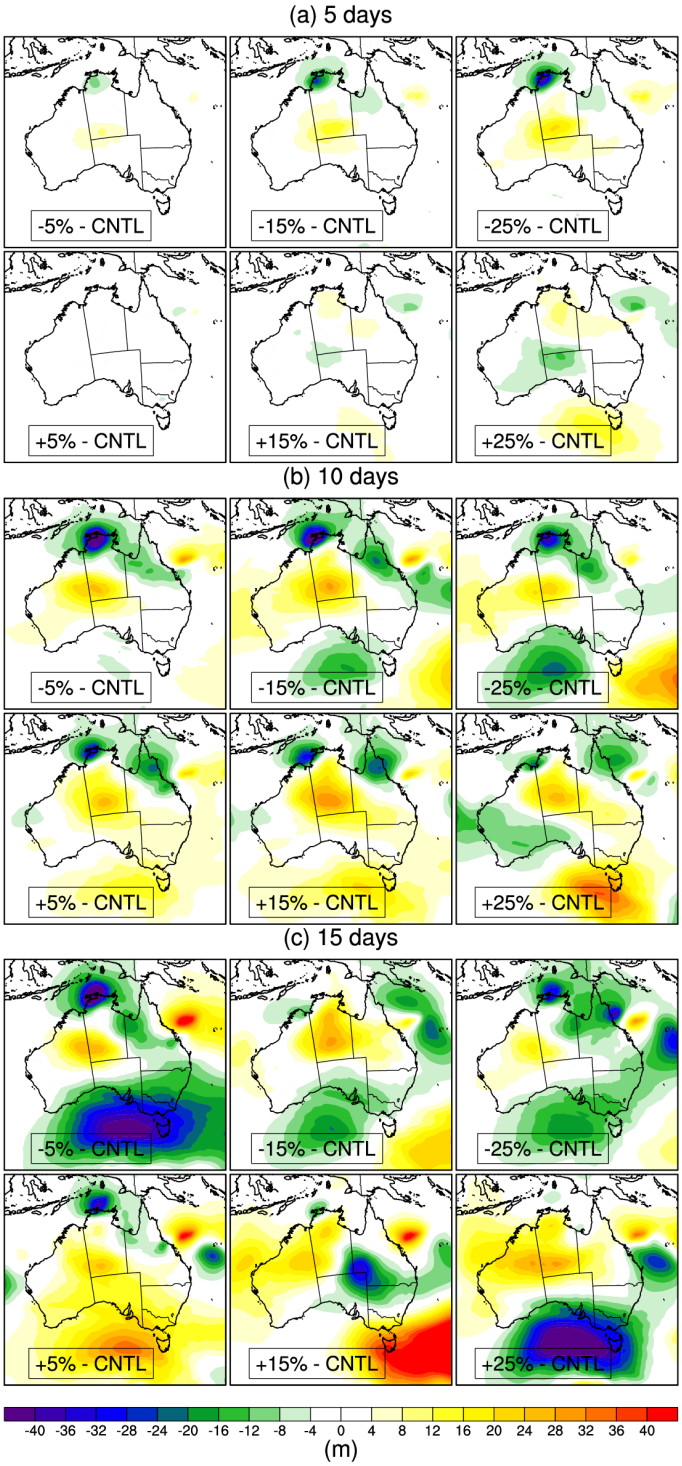

Figure 10. Daily mean difference in 500 hPa geopotential on the 7th of February 2009 between each experiment and the control (experiment-CNTL (Fig. 9)) started at (a) 5 days, (b) 10 days, and (c) 15 days lead time. Positive values indicate that the experiment had higher geopotential height as compare to the CNTL.

Figs. 11 (a) and 12 (a). Over the land, decreasing (increasing) soil moisture results in a decrease (increase) in Q_{le} (Fig. 11 (a)) and broadly, an increase (decrease) in Q_h (Fig. 12 (a)). We note that there are small regions of decrease (increase) in Q_h with decreased (increased) soil moisture, especially when soil moisture is perturbed by a small amount. This can be expected as a relatively small perturbation is less likely to have a persistent effect after 5 days. Overall, the response is consistent and can partly explain the increase (decrease) in 500 hPa GPH over the centre of the continent with decreasing (increasing) soil moisture, consistent with the literature. Over the oceans, there is an increase (decrease) in Q_{le} north of Darwin with decreasing (increasing) soil moisture which corresponds to the intensification (weakening) of the upper-level cyclone over this region (Fig 9), and vice-versa to the northeast of the continent. These changes in Q_{le} over the ocean are driven by, rather than drive the changes in 500 hPa above. This is a result of the "dipole-like" changes in 500 hPa GPH previously discussed.

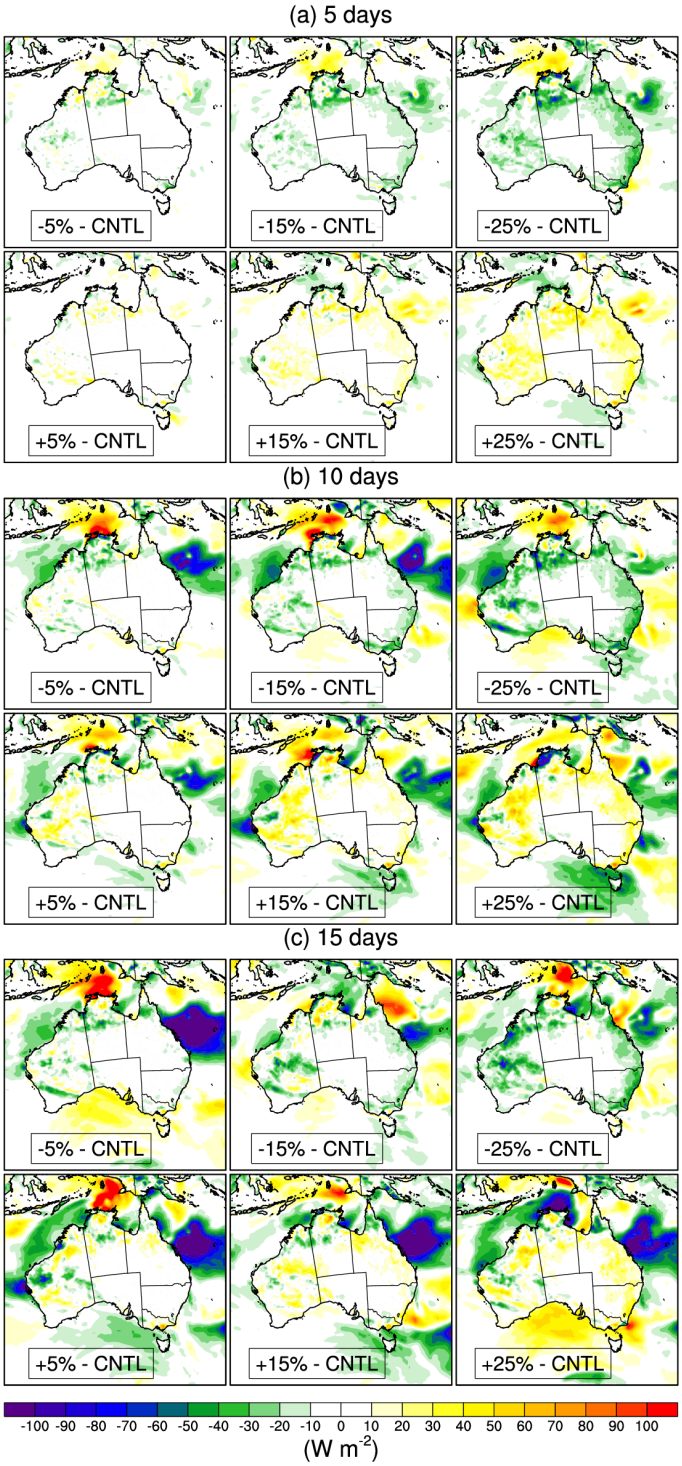

Figure 11. Same as in Figure 10, except showing the change in latent heat flux (Q_{le}, $W\ m^{-2}$).

At 10 days lead time, decreasing initial soil moisture (Fig. 10 (b), top panels) has a similar influence to 5 days lead time (Fig. 10 (a), top panels) with the increase in 500 hPa GPH over the center of the continent and decrease over the Great Australian Bight and northern tropics being more pronounced for 10 days lead time as compared to 5 days lead time. The experiments with increased soil moisture (Fig. 10 (b), bottom panels) also show a similar but stronger increase in 500 hPa GPH over the Great Australian Bight as compared to 5 days lead time (Fig. 10 (a), bottom panels) but the decrease in 500 hPa GPH over the center of the continent is markedly different. Whilst at 5 days lead time, the decrease in 500 hPa GPH is mostly centered over the central southern part of the continent (Fig. 10 (a), bottom panels) at 10 days lead time, the decrease in 500 hPa GPH is almost identical for the +5% and +10% experiments, but markedly intensifies with increasing soil moisture for the +25% experiment from the west-southwestern part of the continent (Fig. 10 (b), bottom panels). As a result, the increase in 500 hPa GPH over the northern part of the

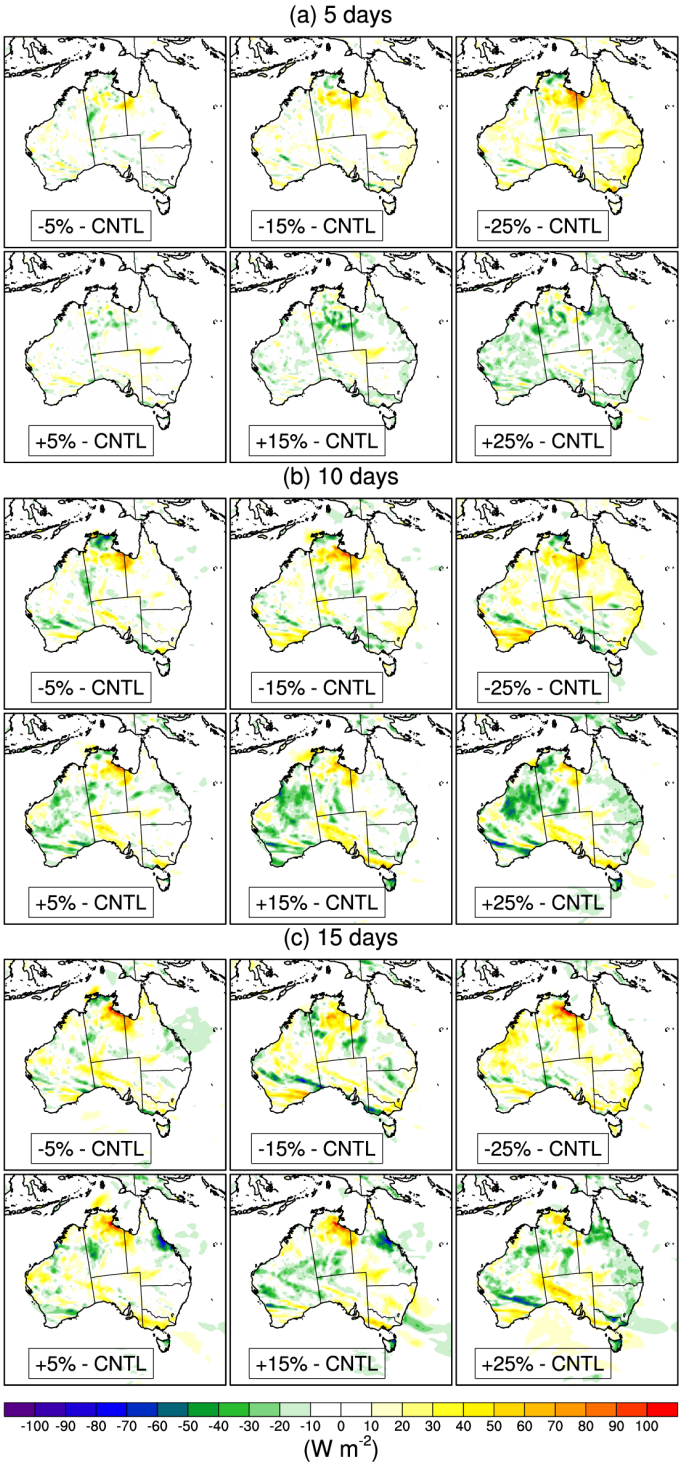

Figure 12. Same as in Figure 10, except showing the change in sensible heat flux (Q_h, W m^{-2}).

continent (Fig 10 (a), bottom panels) extends further south (Fig 10 (b), bottom panels) at 10 days lead time. This can partly explain the changes in TMAX at 10 days lead time for increasing soil moisture (Fig. 7 (b), bottom panels) which showed the decrease in TMAX gradually intensifying from the west-to-southwestern side of the continent and an increase in TMAX over the southeast and central eastern part of the continent. This pattern of increase in 500 hPa GPH to the east and decrease from the west (Fig 10 (b), bottom panels) enhanced the advection of warm continental air from the northwest towards the southeast with differences in the 10 m wind speed over the southeast corner of up to 3 $m\ s^{-1}$ for the +25%-CNTL experiment (not shown).

The changes in Q_{le} (Fig. 11 (b)) over the ocean reflect the changes in 500 hPa GPH (Fig. 10 (b)), with regions of decrease (increase) in 500 hPa GPH showing an increase (decrease) in Q_{le} as expected. Over the land the changes in Q_{le} are broadly consistent with the experiments with decreased (increased) soil moisture showing decreased (increased) Q_{le}. The changes in Q_h

over land however (Fig. 12 (b)), cannot be related to imposed soil moisture perturbation as there are regions of both increases and decreases across the domain, especially for the experiments with increased soil moisture, showing that the imposed perturbation in soil moisture is essentially "lost" after 10 days. The dynamics behind this is explored later in the manuscript.

At 15 days lead time (Fig. 10 (c)), there is no clear pattern in the differences in GPH as compared to 5 and 10 days lead time irrespective of whether soil moisture is increased or decreased, with some patterns being completely opposite. For example, the influence of decreasing soil moisture from -5% to -25% results in a gradual reduction of the increase in GPH over the center of the continent, and a gradual reduction of the decrease in GPH over the Great Australian Bight (Fig. 10 (c), top panels). The experiments with increasing soil moisture show no clear pattern. These changes in GPH are reflected in the changes in Q_{le} (Fig. 11) over the ocean, and similar to the experiments at 10 days lead time, the changes Q_h (Fig. 12) cannot be related to the imposed perturbation in soil moisture.

To better understand these results, we examined the evolution of surface soil moisture for the 15 days lead time experiment as compared to the CNTL, at 5 days, 10 days lead time, and on the day of the event. The imposed increase in soil moisture at 15 days lead time quickly evaporates such that the sign of the change becomes negative over the northern tropics on the day of the event (not shown). Hence, the sign of the imposed perturbation has been lost within 2 weeks. As was shown in Fig. 3, the imposed increase in soil moisture was within $\pm 10\%$ of the field capacity soil moisture over the northern tropics and and any excess soil moisture above field capacity would have been lost via surface runoff.

This is further illustrated by an hourly time series of the difference in soil moisture (Fig. 13) between the experiments and the control (EXPT-CNTL) averaged over the northern tropical region (shown by the brown box in Figure 1), at the different lead times. At 5 and 10 days lead time, the imposed change in soil moisture remains almost constant until the 7th of February 2009 (Fig. 13 (a) and (b), top panels). At 15 days lead time (Fig. 13 (c)), there is a convergence of the difference in soil moisture between the 31st of January and 2nd of February 2009, which is reflected in the change in 2-m temperature (T2). At 5 and 10 days lead time the response of T2 to the soil moisture perturbation is largely linear, whereas at 15 days lead time the response converges to nearly zero between the 31st of January and 2nd of February after which the response has no relation to the imposed initial perturbation. Figure 14 shows the same results but averaged over southeast Australia (shown by the second brown box in Figure 1). The response of T2 to perturbed soil moisture does not vary as smoothly as over the northern tropics (Fig. 13), as the perturbation of soil moisture is smaller over the southeast as compared to the tropics (Fig. 2), but the response at 5 days lead time is broadly consistent (Fig. 14 (a)). At 10 and 15 days lead time (Figs. 14 (b) and (c)), the response of T2 shows little predictability from the imposed perturbation after the 5th and 2nd of February respectively.

We further investigated the mechanisms leading to the lack of predictability over the southeast for the 10 days lead time experiment on the 5th of February. This is illustrated in supplementary Figure S1 showing the 500 hPa GPH from the 3rd to the 6th of February and the difference to the CNTL is shown in Figure S2. The upper-level anticyclone gradually covers most of the continent from the 3rd to the 4th (Fig. S1 (a) and (b)) and intensifies on the 5th, moving eastwards (Fig. S1 (c) and (d)), with the region of highest GPH moving east of the continent on the 7th (Fig. 9 (a)). On the 3rd and the 4th, there is little change in GPH over most of the continent (Figs. S2 (a) and (b)). Between the 5th and the 6th, the increase in GPH to the northeast and decrease over the west for the experiments with increased soil moisture intensifies (Figs. S2 (c) and (d)), eventually leading to the strong gradient in GPH on the 7th (Fig. 10 (b), lower panels). Hence the advection of warm air from the northwest can explain the lack of predictability from the 5th for the 10 days lead time experiment.

The dynamics leading to the lack of predictability for the 15 days lead time experiment around the 2nd of February was different. Between the 31st of January and 3rd of February, a ridge of high pressure parallel to the east coast becomes evident and the upper-level cyclone to the northwest moves towards the southwest (Figure S3). On the 31st of January (Figure S4 (a)), the changes in 500 hPa GPH are mostly confined to the northwest, however, from the 1st to the 3rd of February, there are large reductions in GPH around the southeast coast, especially with the experiments

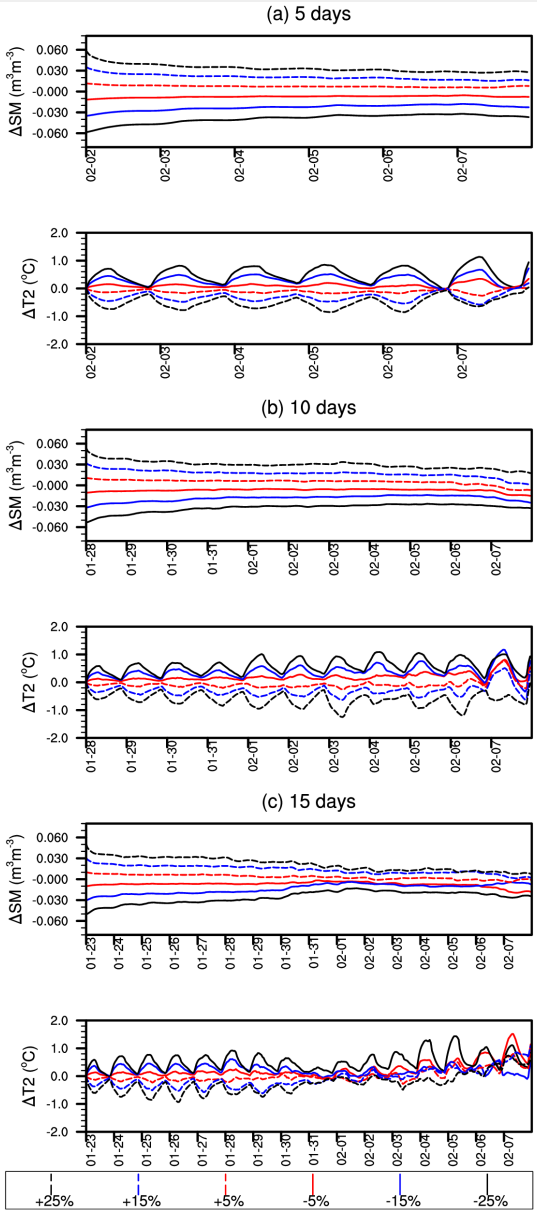

Figure 13. Hourly time series of the difference in surface soil moisture (SM, top panels) and 2m Temperature (T2, bottom panels), between each experiment and the control (experiment-CNTL) over the northern tropics (shown by the brown box in Figure 1) at (a) 5 days, (b) 10 days, and (c) 15 days lead time. Solid lines represent experiments with reduced soil moisture and dotted lines experiments with increased soil moisture. The labelling on the x-axis follows the format of month-day.

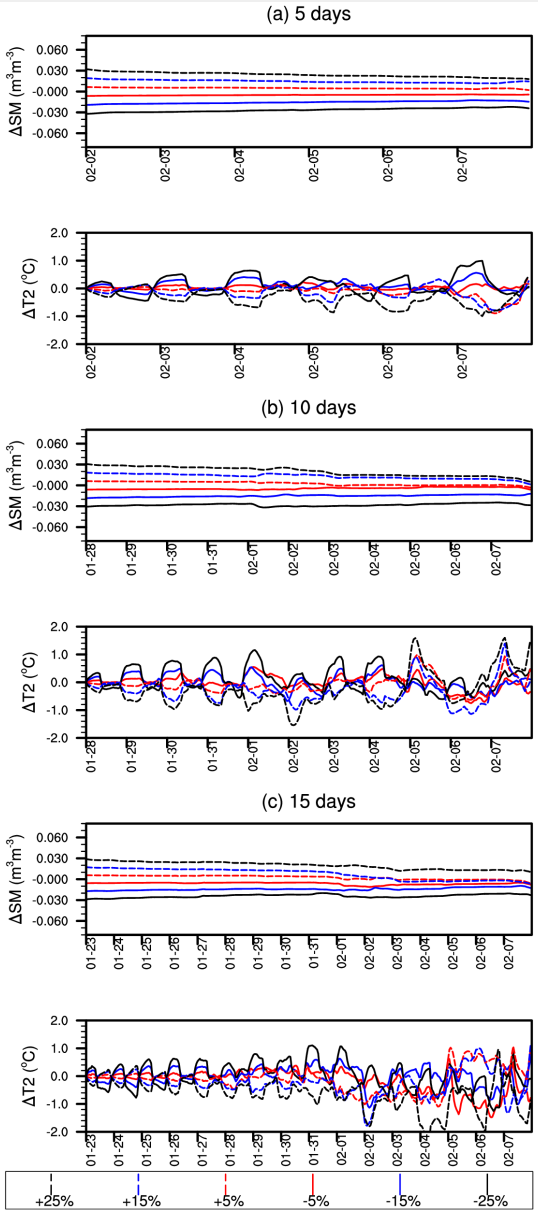

Figure 14. Same as in Figure 13, except averaged over southeast Australia, shown by the box in Figure 1.

with increased soil moisture. After the 3rd, these changes in GPH amplify eventually leading to the large differences shown in Figure 10 (c) on the 7th of February. Hence, for both the 10 and 15 day lead time experiments, a gradual amplification of the changes in the upper-level systems with time, means that the resulting changes in surface meteorology cannot be directly related to the sign of the imposed soil moisture perturbation. Also clearly noticeable in Figure S4 are large changes in the location of the upper-level cyclone to the northwest, especially for the experiments with $\pm$ 25% soil moisture. Decreasing soil moisture changed the location of the cyclone slightly further north whereas increasing soil moisture moved it slightly further south. Given the known teleconnections between tropical cyclone activity and this HW event (Parker *et al.* 2013), it is likely that this can also partly explain the lack of predictability seen in our results.

4. Discussion

Our study differs from previous studies that have investigated the influence of soil moisture on HWs elsewhere in that the perturbation to soil moisture is applied relatively close to the event (up to two weeks). This was deliberate; previous studies have typically fixed soil moisture to a constant value, or prescribed a seasonal cycle (Lorenz *et al.* 2010); perturbed soil moisture up to 2 months prior to the event (Fischer *et al.* 2007; Zampieri *et al.* 2009); used different land surface schemes which either resolve hydrology or prescribe consistently high soil moisture (Stéfanon

et al. 2012); or, initialised soil moisture to fixed values across the domain, ranging from very dry to very wet (Ferranti and Viterbo 2006). For our study, we wanted the soil moisture to still have a realistic spatial pattern; so we choose not to use fixed values. The choice of 15 days was to broadly reflect the time frames usually used in numerical weather prediction.

Our results show that WRF is able to reproduce the HW event reasonably well, although the simulated spatial extent of the HW did not reach as close to the southeast coast as observed with large biases of up to -10°C to -12°C over Victoria. There was a relatively large bias in precipitation over the tropics during the summer months preceding the event. However, comparisons of the simulated surface soil moisture with remotely sensed estimates showed reasonably good spatial agreement facilitating further experiments with perturbed initial soil moisture from the control experiment at varying lead times.

At short lead times of 5 days, decreasing (increasing) soil moisture led to an increase (decrease) in maximum temperature, due to an intensification of upper-level highs. This is consistent with earlier literature (Fischer *et al.* 2007; Zampieri *et al.* 2009). At longer lead times of 10 and 15 days, the influence of perturbing soil moisture becomes more non-linear, especially when soil moisture is increased rather than reduced. Over a semi-arid continent such as Australia, a reduction in soil moisture essentially makes a dry continent slightly drier, and an increase in soil moisture is likely to be quickly lost via surface evaporation. As a result, over relatively long lead times, the response on the day cannot be easily related to the imposed perturbation 10 to 15 days prior. Nonetheless, we further explored the dynamical reasons leading to the lack of predictability.

At 10 days lead time, we showed that the unexpected increase in TMAX over the center of the continent and the southeast with increase in soil moisture was due to the patterns of 500 hPa GPH leading to the advection of warm continental air from the northwest to the southeast. Hence, even small changes in soil moisture have an influence on upper-level anticyclone and the resulting interactions with surrounding cyclones can result in large changes in the spatial extent of TMAX over the continent. The control simulation showed a negative bias in TMAX over the southeast and an under-estimation of precipitation over the tropics when compared with gridded observations. This translated into an under-estimation of soil moisture over the tropics when compared with remotely sensed estimates. The experiments with higher soil moisture can therefore be regarded as having soil moisture closer to reality. These experiments showed increases in TMAX over southeast, where the CNTL had a large negative bias. Hence, the experiments with increased soil moisture provide a plausible explanation (increased continental warm air advection) for the large under-estimation of TMAX by WRF (CNTL) over the southeast.

For the 15 days lead time experiment, we showed that between the 31st of January and 3rd of February, changes in GPH were large enough to alter a ridge of high pressure on the east coast. These changes amplified such that it was not possible to relate them to the imposed sign of the perturbation in soil moisture. Hence, beyond 10 days lead time, perturbing soil moisture has little impact on the predictability of the event as the changes in the upper-level systems become too large and essentially override the imposed change in soil moisture. This is an important result as it shows that accurate surface soil moisture is critical in the simulating of HW events such as the Black Saturday bushfires, but the predictability of the effect of soil moisture is only possible up to 5 to 10 days prior to the event. Parker *et al.* (2013) showed strong links between tropical cyclone activity to the northwest and the Black Saturday bushfires, and our results at the 15 day lead time showed a slight shift in the position of the tropical cyclone to the northwest with soil moisture perturbations. Hence this is also likely a contributing factor to the lack of predictability.

The role of soil moisture in determining the predictability of maximum temperatures over Australia has been documented elsewhere. For example, Timbal *et al.* (2002) ran simulations over Australia with freely evolving soil moisture versus a prescribed climatology, and showed that it is not possible to capture atmospheric variability over Australia without resolving soil moisture variability. Similarly, Hirsch *et al.* (2014) have shown that realistic initial soil moisture conditions improves the predictability of maximum temperatures over Australia, especially at short lead times of up to 16-30 days. This is consistent with the results presented here. We showed that even slightly different initial ($\pm$ 5%, $\pm$15%) conditions 15 days in advance of an event

led to differences in maximum temperatures exceeding 1°C to 2°C. The event considered here was one of the most significant HW events in Australian history; hence our results show higher sensitivity than other studies that have typically focused on seasonal means (Hirsch *et al.* 2014).

5. Conclusions

The climatology and large-scale drivers of HW events in Australia is well documented, as are future climate projections of HWs over Australia. However, the role of soil moisture on HW dynamics in Australia remains largely unexplored and a large body of literature on HW events elsewhere suggests it plays a key role. We addressed this gap by conducting a series of experiments with perturbed initial soil moisture up to ± 5%, ± 15%, and ± 25%, at 5, 10, and 15 days lead time to one of the most significant bushfires/HW events in southeast Australia, the Black Saturday bushfires. The focus of the paper was on the influence soil moisture perturbations at the synoptic/continental scale.

Our results show that soil moisture has an important role in modulating the intensity of HW events in southeast Australia. We show that the impact of perturbing soil moisture is strongly dependent on lead time to the event. At 5 days lead time, decreasing (increasing) soil moisture, increases (decreases) maximum temperature over most of the continent, via an intensification of upper-level highs. At longer lead times of 10 to 15 days, the imposed perturbation is essentially lost, and the resulting impact on maximum temperature on the day of the event has no predictability as the changes in the upper-level systems become too large. This highlights that accurate initial soil moisture profiles are essential to capturing the severity and spatial occurrence of HWs in southeast Australia. More importantly, soil moisture in the tropics is shown to have a strong influence on HW dynamics in southeast Australia. Hence, whilst HW events in southeast Australia are largely driven at the large scale, soil moisture is critical in modulating their spatial extent and magnitude, but this relationship only predictable at relatively short lead times.

6. Supplementary information

Figure S1: Mean daily 500 hPa geopotential height (GPH) from the CNTL experiment, from the 3rd to the 6th of February 2009.

Figure S2: Difference in 500 hPa geopotential height between each experiment and the CNTL for the experiment at 10 days lead time, from the 3rd to the 6th of February 2009.

Figure S3: Mean daily 500 hPa geopotential height (GPH) from the CNTL experiment, from the 31st of January to the 3rd of February 2009.

Figure S4: Difference in 500 hPa geopotential height between each experiment and the CNTL for the experiment at 15 days lead time, from the 31st of January to the 3rd of February 2009.

Acknowledgement

This work was supported by the Australian Research Council Centre of Excellence for Climate System Science (CE110001028) and the NSW Environment Trust (RM08603). Evans was supported by the Australian Research Council through the Future Fellowship FT110100576. We thank the National Computational Infrastructure at the Australian National University, an initiative of the Australian Government, for access to supercomputer resources. The AMSR_E soil moisture data was provided by Yi Liu from the University of New South Wales Climate Change Research Center. ECMWF ERA-Interim data used in this study/project have been provided by ECMWF/have been obtained from the ECMWF Data Server. The comments of two anonymous reviewers helped to improve the manuscript. All this assistance is gratefully acknowledged.

References

Andrys J, Lyons TJ, Kala J. 2015. Multi-decadal evaluation of WRF downscaling capabilities over Western Australia in simulating rainfall and temperature extremes. *Journal of Applied Meteorology and Climatology* **54**: 370–394, doi:10.1175/JAMC-D-14-0212.1.

Boschat G, Pezza A, Simmonds I, Perkins S, Cowan T, Purich A. 2014. Large scale and sub-regional connections in the lead up to summer heat wave and

extreme rainfall events in eastern Australia. *Climate Dynamics, in press* doi:10.1007/s00382-014-2214-5.

Cai W, Cowan T, Raupach M. 2009. Positive Indian Ocean Dipole events precondition southeast Australia bushfires. *Geophysical Research Letters* **36**: L19 710, doi:10.1029/2009GL039902.

Cowan T, Purich A, Perkins S, Pezza A, Boschat G, Sadler K. 2014. More frequent, longer, and hotter heat waves for Australia in the twenty-first century. *Journal of Climate* **27**: 5851–5871, doi:10.1175/JCLI-D-14-00092.1.

Dee DP, Uppala SM, Simmons AJ, Berrisford P, Poli P, Kobayashi S, Andrae U, Balmaseda MA, Balsamo G, Bauer P, Bechtold P, Beljaars ACM, van de Berg L, Bidlot J, Bormann N, Delsol C, Dragani R, Fuentes M, Geer AJ, Haimberger L, Healy SB, Hersbach H, Hólm EV, Isaksen L, Kållberg P, Köhler M, Matricardi M, McNally AP, Monge-Sanz BM, Morcrette JJ, Park BK, Peubey C, de Rosnay P, Tavolato C, Thépaut JN, Vitart F. 2011. The ERA-Interim reanalysis: configuration and performance of the data assimilation system. *Quarterly Journal of the Royal Meteorological Society* **137**: 553–597, doi:10.1002/qj.828.

Ek MB. 2003. Implementation of Noah land surface model advances in the National Centers for Environmental Prediction operational mesoscale Eta model. *Journal of Geophysical Research* **108**(D22): 8851, doi:10.1029/2002JD003296.

Engel CB, Lane TP, Reeder MJ, Rezny M. 2013. The meteorology of Black Saturday. *Quarterly Journal of the Royal Meteorological Society* **139**: 585–599, doi:10.1002/qj.1986.

Evans JP, Ekstrom M, Ji F. 2012. Evaluating the performance of a WRF physics ensemble over South-East Australia. *Climate Dynamics* **39**: 1241–1258, doi:10.1007/s00382-011-1244-5.

Evans JP, McCabe MF. 2010. Regional climate simulation over Australia's Murray-Darling basin: A multitemporal assessment. *Journal of Geophysical Research* **115**: D14 114, doi:10.1029/2010JD013816.

Evans JP, Westra S. 2012. Investigating the mechanisms of diurnal rainfall variability using a regional climate model. *Journal of Climate* **25**: 7232–7247, doi:10.1175/JCLI-D-11-00616.1.

Ferranti L, Viterbo P. 2006. The European summer of 2003: Sensitivity to soil water initial conditions. *Journal of Climate* **19**: 3659–3680, doi:10.1175/JCLI3810.1.

Fischer EM, Seneviratne SI, Vidale PL, Lüthi D, Schär C. 2007. Soil moisture-atmosphere interactions during the 2003 European summer heat wave. *Journal of Climate* **20**: 5081–5099, doi:10.1175/JCLI4288.1.

Giorgi F, Jones C, Asrar GR. 2009. Addressing climate information needs at the regional level: the CORDEX framework. *World Meteorological Organization Bulletin* **58**: 175–183.

Hirsch AL, Kala J, Pitman AJ, Carouge C, Evans JP, Haverd V, Mocko D. 2014. Impact of land surface initialization approach on subseasonal forecast skill: A regional analysis in the southern hemisphere. *Journal of Hydrometeorology* **15**: 300–319, doi:10.1175/JHM-D-13-05.1.

Hirschi M, Seneviratne SI, Alexandrov V, Boberg F, Boroneant C, Christensen OB, Formayer H, Orlowsky B, Stepanek P. 2010. Observational evidence for soil-moisture impact on hot extremes in southeastern Europe. *Nature Geoscience* **4**: 17–21, doi:10.1038/ngeo1032.

Jacobs SJ, Vihma T, Pezza AB. 2014. Heat stress during the Black Saturday event in Melbourne, Australia. *International Journal of Biometeorology* doi:10.1007/s00484-014-0889-2.

Jones DA, Trewin BC. 2000. On the relationships between the El-Nino-Southern-Oscillation and Australian land surface temperature. *International Journal of Climatology* **20**: 697–719.

Jones DA, Wang W, Fawcett R. 2009. High-quality spatial climate data-sets for Australia. *Australian Meteorological and Oceanographic Journal* **58**: 233.

Kala J, Andrys J, Lyons TJ, Foster IJ, Evans BJ. 2015. Sensitivity of WRF to driving data and physics options on a seasonal time-scale for the southwest of Western Australia. *Climate Dynamics* **44**: 633–659, doi:10.1007/s00382-014-2160-2.

Lau WKM, Kim KM. 2012. The 2010 Pakistan flood and Russian heat wave: Teleconnection of hydrometeorological extremes. *Journal of Hydrometeorology* **13**: 392–403, doi:10.1175/JHM-D-11-016.1.

Liu YY, van Dijk AIJM, de Jeu RAM, Holmes TRH. 2009. An analysis of spatiotemporal variations of soil and vegetation moisture from a 29-year satellite-derived data set over mainland Australia. *Water Resources Research* **45**: W07 405, doi:10.1029/2008WR007187.

Lorenz R, Jaeger EB, Seneviratne SI. 2010. Persistence of heat waves and its link to soil moisture memory. *Geophysical Research Letters* **37**: L09 703, doi:10.1029/2010GL042764.

Marshall AG, Hudson D, Wheeler MC, Alves O, Hendon HH, Pook MJ, Risbey JS. 2014. Intra-seasonal drivers of extreme heat over Australia in observations and POAMA-2. *Climate Dynamics* **43**: 1915–1937, doi:10.1007/s00382-013-2016-1.

Martius O, Sodemann H, Joos H, Pfahl S, Winschall A, Croci-Maspoli M, Graf M, Madonna E, Mueller B, Schemm S, Sedlek J, Sprenger M, Wernli H. 2013. The role of upper-level dynamics and surface processes for the Pakistan flood of July 2010: Dynamics and Surface Processes of the Pakistan Flood in 2010. *Quarterly Journal of the Royal Meteorological Society* **139**: 1780–1797, doi:10.1002/qj.2082.

Miralles DG, Teuling AJ, van Heerwaarden CC, Vilà-Guerau de Arellano J. 2014. Mega-heatwave temperatures due to combined soil desiccation and atmospheric heat accumulation. *Nature Geoscience* **7**: 345–349, doi:10.1038/ngeo2141.

Nicholls N, Larsen S. 2011. Impact of drought on temperature extremes in Melbourne, Australia. *Australian Meteorological and Oceanographic Journal* **61**: 113–116.

Parker TJ, Berry GJ, Reeder MJ. 2013. The influence of tropical cyclones on heatwaves in southeastern Australia. *Geophysical Research Letters* **40**: 6264–6270, doi:10.1002/2013GL058257.

Parker TJ, Berry GJ, Reeder MJ. 2014a. The structure and evolution of heat waves in southeastern Australia. *Journal of Climate* **27**: 5768–5785, doi: 10.1175/JCLI-D-13-00740.1.

Parker TJ, Berry GJ, Reeder MJ, Nicholls N. 2014b. Modes of climate variability and heat waves in Victoria, southeastern Australia. *Geophysical Research Letters* **41**: 6926–6934, doi:10.1002/2014GL061736.

Pezza AB, Rensch P, Cai W. 2011. Severe heat waves in southern Australia: Synoptic climatology and large scale connections. *Climate Dynamics* **38**: 209–224, doi:10.1007/s00382-011-1016-2.

Purich A, Cowan T, Cai W, van Rensch P, Uotila P, Pezza A, Boschat G, Perkins S. 2014. Atmospheric and oceanic conditions associated with southern Australian heat waves: A CMIP5 analysis. *Journal of Climate* **27**: 7807–7829, doi:10.1175/JCLI-D-14-00098.1.

Skamarock WC, Klemp JB, Dudhia J, Gill DO, Barker DM, Duda Michael G, Huang XY, Wang W, Powers JG. 2008. A description of the advanced research WRF version 3. URL http://www2.mmm.ucar.edu/wrf/users/docs/arw_v3.pdf.

Stéfanon M, Drobinski P, D'Andrea F, de Noblet-Ducoudré N. 2012. Effects of interactive vegetation phenology on the 2003 summer heat waves. *Journal of Geophysical Research* **117**: D24 103, doi:10.1029/2012JD018187.

Teague B, McLeod R, Pascoe S. 2010. 2009 Victorian bushfires Royal Comission, Final Report. URL http://www.royalcommission.vic.gov.au/Commission-Reports.html.

Timbal B, Power S, Colman R, Viviand J, Lirola S. 2002. Does soil moisture influence climate variability and predictability over Australia? *Journal of Climate* **15**: 1230–1238.

Zampieri M, D'Andrea F, Vautard R, Ciais P, de Noblet-Ducoudré N, Yiou P. 2009. Hot European summers and the role of soil moisture in the propagation of Mediterranean drought. *Journal of Climate* **22**: 4747–4758, doi:10.1175/2009JCLI2568.1.

